A hybrid method for determination of fatigue limit and non-destructive evaluation of composite structures after low-velocity impact loading

Andrzej Katunin, Ivanna Pivdiablyk, Laurent Gornet, Patrick Rozycki

Composites Part B 238 (2022) 109898

Contents lists available at ScienceDirect

Composites Part B

journal homepage: www.elsevier.com/locate/compositesb

A hybrid method for determination of fatigue limit and non-destructive evaluation of composite structures after low-velocity impact loading

Andrzej Katunin [a,*], Ivanna Pivdiablyk [b], Laurent Gornet [b], Patrick Rozycki [b]

[a] Department of Fundamentals of Machinery Design, Faculty of Mechanical Engineering, Silesian University of Technology, Konarskiego 18A, 44-100, Gliwice, Poland
[b] Research Institute in Civil and Mechanical Engineering (GeM), Ecole Centrale de Nantes, 1 Rue de la Noë, 44300, Nantes, France

ARTICLE INFO

Keywords:
Polymer-matrix composites (PMCs)
Fatigue
Impact behaviour
Non-destructive testing

ABSTRACT

One of the most challenging and still unsolved problems within the design and operation of composite structures is the prediction of its behavior under fatigue loading. This problem is even more complex when a composite structure contains damage, especially low-velocity impact damage considered as one of the most dangerous types of damage in composite structures. In this paper, the authors presented the hybrid method, which combines the evaluation of a fatigue limit of structures with low-velocity impact damage (LVID) with a non-destructive evaluation of this damage using thermocouples and thermography in a single test. The tests were performed on carbon and glass fiber-reinforced composite structures with LVID of various energies. The relation between fatigue limit and impact energy was demonstrated, and the observed damage mechanisms analysis was performed. Moreover, the performance of LVID detectability is analyzed, defining minimal self-heating temperature increase necessary for detection of LVID. The proposed method demonstrated high sensitivity to impact damage and simultaneously an ability of evaluation of fatigue life of a tested structure. Finally, the recommendations on measurement setup and parameters of testing are provided. It was demonstrated that the proposed hybrid method could be successfully used for rapid, precise and non-destructive evaluation of residual life of composite structures after impact loading.

1. Introduction

A structural residual life of composites is one of the key parameters for designing and operating structures and elements in various industrial branches. Considering that the fatigue life prediction of composites is a still-unsolved problem and a significant challenge, the demand for effective residual life evaluation methods is high. However, due to the high complexity of the internal architecture of composite materials and numerous interactions between particular constituents in their compositions, as well as the high impact of manufacturing parameters, prediction of their residual life using the concepts of continuum mechanics poses a big challenge; thus, numerous approaches developed to-date are focused on purely experimental studies or a mixture of experimental, numerical, and theoretical studies [1–5]. In some cases, the thermodynamic modeling of fatigue limit for predicting a structural residual life allowed achieving high compliance with the experimental results (see e.g. Ref. [6]).

Within the methods of evaluating structural residual life, one of the popular approaches is based on the fatigue limit concept, which provides information on critical damage accumulation in a tested composite structure leading to irreversible changes and propagating damage. What is essential to notice, this concept allows evaluating a structural residual life in a non-destructive way based on a slope of a function of applied stress and response in the form of an amount of dissipated heat. Several methods of a fatigue limit evaluation developed to-date were summarized in Ref. [7]. The studies on evaluation of a fatigue limit were firstly developed for metals [8–16] and further adapted to polymer matrix composites (PMCs) [17–28]. It is worth mentioning that the heat generation mechanisms are different in both cases [29]: for metals, the governing mechanism is plasticity, while in the case of polymers and PMCs, the heat generation process is driven mainly by the viscoelastic response, and the resulting behavior is called the self-heating effect. This effect results from a conversion of mechanical energy to thermal due to the viscoelastic behavior of polymers and PMCs. As the previous research results show [30], it may cause intensive and accelerated degradation even in the case of a low self-heating temperature increase. Therefore, it is necessary to validate that the loading for fatigue limit determination tests does not affect

* Corresponding author.
E-mail address: andrzej.katunin@polsl.pl (A. Katunin).

https://doi.org/10.1016/j.compositesb.2022.109898
Received 7 January 2022; Received in revised form 11 March 2022; Accepted 11 April 2022
Available online 14 April 2022

irreversible changes in the tested structures and to confirm the non-destructivity of the testing approach, which is often omitted in the studies related to fatigue life evaluation. In the previous studies [31–33], such validation was performed based on the critical self-heating temperature value, which was considered as a kind of material property, barely dependent on the loading parameters in fatigue tests. A combination of the critical self-heating temperature with the fatigue limit was proposed in Ref. [34].

From the point of view of PMC structures operation, it is essential to evaluate their residual life in the case of appearance of a defect or damage and appropriately plan their further operation. In numerous industrial branches, like aircraft, automotive, naval or nuclear, the various non-destructive testing (NDT) methods, including ultrasonic testing, infrared thermography, radiography and computed tomography, vibroacoustic testing, eddy current and magneto-optical testing, terahertz spectroscopy and numerous optical methods, like electronic speckle pattern interferometry and shearography, and many others are widely used for inspection purposes. A comprehensive overview of these methods can be found e.g. in Ref. [35]. However, connecting the inspection results with the remaining structural life is a challenging task, which is currently under investigation by numerous research teams [36–38].

The problem of evaluating a residual life using the self-heating approach, becomes more complicated, mainly when a tested structure contains a defect or damage. With respect to the classical testing approach, including Luong's method and derivative methods based on fitting stress-temperature points using non-linear functions (see Ref. [7] for more details), the presence of spots with critical stress requires the local measurements of the self-heating temperature to obtain its highest values. This problem was considered in very few studies. Karama [17] and Wang et al. [39] investigated the fatigue limit of specimens with holes using infrared thermography (IRT), and the resulting thermograms clearly show the hot spots in the location of a hole in both studies. Foti et al. [40] analyzed pre-notched specimens and reported that the maximal self-heating temperature was observed in a vicinity of an introduced notch. Similar observations were made by the authors of [41, 42], where they used IRT for monitoring the evolution of structural damage in PMC structures with barely visible impact damage (BVID) during fatigue loading. Butler et al. [43] investigated PMC structures with BVID based on an analytical approach of a fatigue limit determination. The authors stated that the development of initial delamination, represented by BVID, is a driving mechanism for its further propagation, which coincides with the previously discussed observations for specimens with holes. Nevertheless, there is a lack of systematic studies on the evaluation of a fatigue limit of damaged PMC structures.

Low-velocity impact damage (LVID) is one of the damage types, which attracts the attention of numerous industrial branches, primarily aircraft and aerospace industries. It is due to the ability of propagation of the resulting delamination (especially in carbon fiber-reinforced polymeric (CFRP) composites – see e.g. Refs. [44,45]), and simultaneously, difficulties with its detection resulting from bare visibility in most cases. In particular, the extent of the propagation of the delamination for a given lamina depends on the depth of the lamina from the point of impact [45]. Nevertheless, the effectiveness of LVID detection using various NDT techniques, including IRT, was confirmed in numerous studies (see e.g. Refs. [38,46–50]). From a practical perspective, IRT generates a thermogram that can represent overall LVID more unambiguously than the other well-known NDT method, namely ultrasound testing in C-Scan mode, and thus IRT is a useful method for quantitative studies [50]. Recent developments on the incorporation of the self-heating effect resulted in the development of the new NDT method – the self-heating based vibrothermography (SHVT), which was successfully employed in NDT of PMC structures with various types of defects, including simulated cracks, flat bottom holes [51,52], and LVID [53].

The paper aims to present the developed hybrid approach, which combines the advantages of precise, non-destructive and rapid evaluation of a fatigue limit of PMCs with impact damage with a simultaneous non-destructive estimation of impact damage extent. The proposed method allows for a comprehensive evaluation of a condition of a tested structure and connection of a damage extent to a remaining structural life. The method was tested on CFRP and glass fiber-reinforced polymeric (GFRP) composites with four levels of impact loading. Numerous technical questions, including the recommendations on measurement setup and procedure as well as the selection of thermograms, are given in the paper.

2. Materials and testing procedures

2.1. Tested composites

The tests were performed on CFRP and GFRP rectangular specimens with a length of 150 mm, a width of 25 mm and a thickness of 2 ± 0.2 mm. The CFRP specimens were purchased from the Dexcraft s.c. (Helenów, Poland), while the GFRP specimens were purchased from the Izo-Erg S.A. (Gliwice, Poland) in the form of longer coupons, which were then cut to a specific length. In both cases, the plain weave fabric (carbon and glass, respectively) was used to reinforce the considered composites. The manufacturing details of the specimens can be found in Refs. [38,54]. The material properties of the composites being of interest in this study were determined in previous experiments and are presented in Table 1.

2.2. Impact damage

Impact damage was introduced to the tested specimens using the in-house drop weight testing machine, designed and constructed at the Department of Fundamentals of Machinery Design, Silesian University of Technology (see Fig. 1(a)). More information on the impact testing machine can be found in Ref. [53]. The specimens were glued with a double-sided adhesive tape to a thick GFRP plate fixed by holders, and the impact energy was defined in the dedicated software of the testing machine. For each impact energy value, the height and mass of an impact platform were automatically calculated, and the impact was performed. The impactor used in this study has a diameter of 34 mm, a total length of 68 mm, and its tip was a cone with a sharp end ($R < 1$ mm) and a slant angle of 45°. To prevent rebounding of the impactor, two electromagnets were activated when the encoders located on both sides of the impacting platform detected a change in the direction of movement and intercepted the impacting platform. The impact tests were performed with the conical steel impactor and predefined impact energies of 10J, 20J, 30J and 40J. The impact energies were selected based on the preliminary tests to obtain all types of impact damage: starting with BVID, which does not cause noticeable damage on front and back surfaces of a specimen (except damage resulting from the indentation of impactor), and ending with the extensive impact damage, which significantly affects local mechanical properties, but does not cause structural disintegration. Impact damage was always located in the geometric center of a specimen. Three specimens were tested for each unique set of parameters to ensure the repeatability of the obtained results. It gives 24 specimens in total considered in this study. The view of the impacted specimens with various energies is presented in Fig. 1 (b).

Table 1
Material properties of the tested specimens [38,54].

	CFRP	GFRP
Elastic modulus at tension, MPa	55017	28500
Ultimate tensile strength, MPa	542.91	413.00

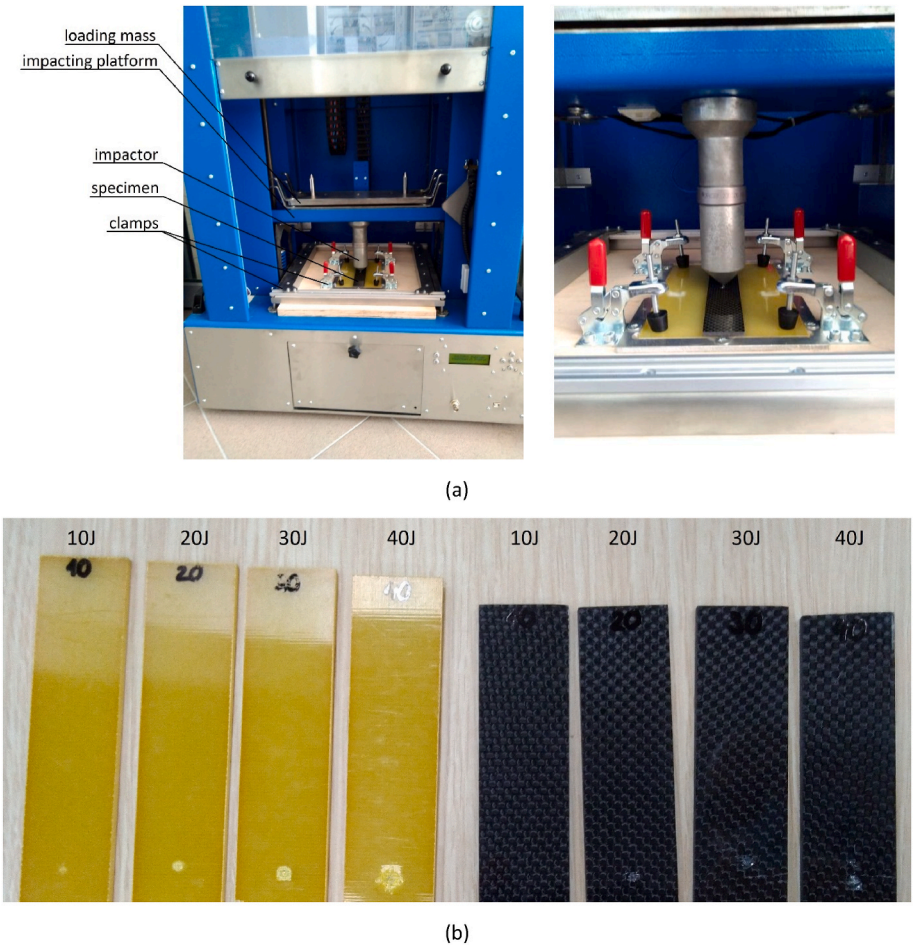

Fig. 1. The drop weight testing machine during introducing LVID (a) and the selected tested specimens after the introduction of impact damage with marked ascending impact energies (b).

2.3. Fatigue limit testing

The specimens with introduced impact damage were then subjected to tensile fatigue loading in the fluctuating tension mode (R = 0.1) on the Instron® ElectroPuls™ E10000 dynamic testing machine at the Research Institute in Civil and Mechanical Engineering, Centrale Nantes. Prior to testing, a front surface of each specimen was covered with the Rust-Oleum® black matt paint ref. 2178 (see Fig. 2(a)) to ensure appropriate emissivity during IRT testing. Moreover, six RS Pro type K thermocouples (ø1/0.2 mm, max. temperature sensed 260 °C) were

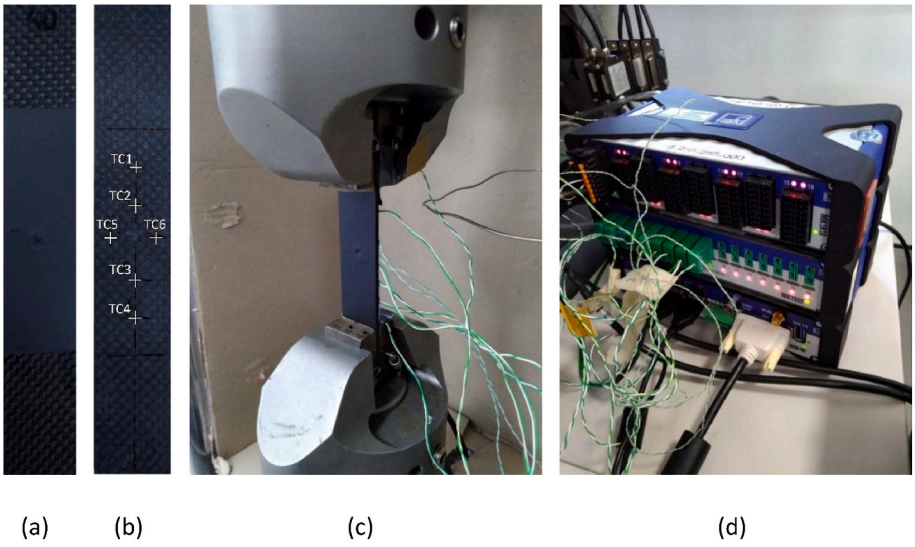

Fig. 2. Preparation for the fatigue experiments: (a) the exemplary specimen covered with paint, (b) configuration of measurement points for thermocouples, (c) the specimen mounted in grips, (d) DAQ for thermocouples.

glued using adhesive tape to a back surface of each specimen before testing in the configuration presented in Fig. 2(b). The distances between particular measurement points were as follows: points *TC2*, *TC3*, *TC5*, and *TC6* were located at 7.5 mm from the center of impact damage, while points *TC1* and *TC4* at the distance of 15 mm from the same origin. The thermocouples were used to evaluate the differences in temperature distribution from the backside of specimens using fatigue limit tests. The specimens prepared in such a way were mounted in the grips of the testing machine with additional pads made of sandpaper to ensure appropriate fixing during fatigue tests. The specimen mounted in grips is presented in Fig. 2(c). The thermocouples were connected to the HBM® QuantumX data acquisition (DAQ) system through the MX1609 thermocouple amplifier (see Fig. 2(d)). Besides the thermocouples glued directly to the specimen, several other locations were subjected to temperature measurements, namely the upper and lower grip of the mechanical testing machine as well as a thermocouple used for the measurement of ambient temperature. The temperature measurements were managed through the HBM® catman®Easy software dedicated to the DAQ system.

The fatigue testing program was designed in the Instron® dedicated software to the mechanical testing machine. After performing preliminary tests for evaluation of maximal force of loading at particular loading levels as well as loading frequency, the following parameters were set for the performed fatigue tests. The loading frequency of 40 Hz was selected to achieve a measurable level of generated heat. The number of cycles within a single level was set to 30000, corresponding to a loading duration of 12.5 min.

According to the results of preliminary tests, such a duration made it possible to stabilize the self-heating temperature for particular loading levels. Subsequently, the duration of unloading between the loading blocks was set to 5 min, which was necessary for stabilizing the temperature of a tested specimen at the ambient temperature level. 14 loading levels were defined for fatigue testing to ensure good approximation capability during the determination of the fatigue limit from the stress-temperature plots, which resulted in a total duration of a single test of 245 min. The maximal force for CFRP and GFRP specimens was defined based on preliminary tests and using the rule that the maximal stress values should be proportional to the elastic moduli of particular materials. Considering that the tested specimens contained LVID, it is assumed that the maximal stress at the highest loading level should be ca. 0.35% of the elastic modulus at tension (see Table 1). Analysing thermal response during preliminary tests as well as results obtained in previous studies (see, e.g., Refs. [30,32–34,51–53]), the selected value of the highest loading stress makes it possible to classify the proposed method as non-destructive. The stress values for particular loading levels for both materials are presented in Table 2.

Additionally, to perform temperature measurements on the front surface of tested specimens and evaluate the detectability of impact damage, the InfraTec® ImageIR® 5310 infrared (IR) camera was used. The thermograms were registered with a framerate of 1 frame per second using a resolution of the acquired thermograms of 320 × 256 pixels. The acquisition was performed via the InfraTec® IRBIS® 3 dedicated software. The acquisition parameters of thermograms were as follows: distance to the tested specimen 0.5 m, emissivity 0.9, environmental temperature 23 °C. To avoid thermal reflections, the surrounding of a tested specimen was covered with cardboard. The maximal temperature registered on the specimen's surface was considered in further studies. The measurements of all the above-discussed parameters were performed synchronously. The whole experimental setup of fatigue tests is presented in Fig. 3.

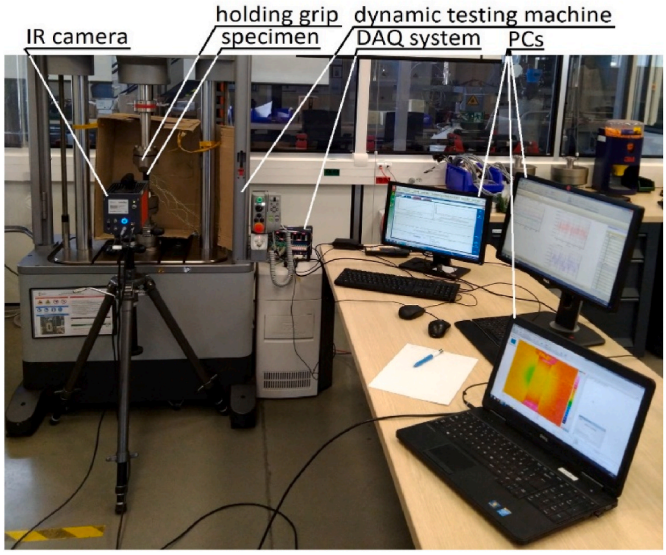

Fig. 3. The experimental setup of fatigue tests.

3. Results on the fatigue limit of impacted structures and identification of damage

3.1. Influence of impact damage on the fatigue limit

The fatigue limit of the tested specimens was determined using the temperature measurements both with thermocouples and IRT. The general evaluation of the fatigue limit was based on IRT, while the analysis of a possible substitution of IRT measurements with a set of thermocouples was provided in the following subsection. After acquiring the sequences of thermograms, the maximal self-heating temperature was determined in each thermogram within a considered sequence, and the time history plot was generated in the IRBIS® software and then exported to text files. These files were then imported into Matlab® 2019b environment for further processing.

The temperature correction was applied to the obtained maximal self-heating temperature waveforms from IRT measurements in the first step of processing. This correction was necessary due to the observed fluctuations of an ambient temperature during loading blocks. For this purpose, the waveform of an ambient temperature registered by one of the thermocouples was subtracted from the maximal self-heating temperature waveform for each considered specimen. Further, the corrected self-heating temperature waveforms were subjected to smoothing in order to limit temperature fluctuations observed during IRT measurements. For filtering, a Savitzky-Golay filter with the empirically determined polynomial order of 20 and a window width of 351 was applied to the temperature waveforms. The exemplary waveform after the above-described processing steps is presented in Fig. 4.

Based on the obtained plots, an automatic routine was developed to identify the limit points of particular loading blocks, which correspond to the maximal self-heating temperature registered for these blocks. For this purpose, the maximal self-heating temperature history was time-synchronized with the loading history. The obtained values of the maximal self-heating temperature for each loading block within a given test were plotted against the applied stress levels to determine the fatigue limit following Luong's method [8]. This method is based on interpolating the experimental results by two lines and determining the

Table 2
The applied stress levels at the defined loading blocks to the tested specimens.

CFRP, MPa	36	48	60	72	84	96	108	120	132	144	156	168	180	192
GFRP, MPa	12	18	24	30	36	42	48	54	60	66	72	78	84	90

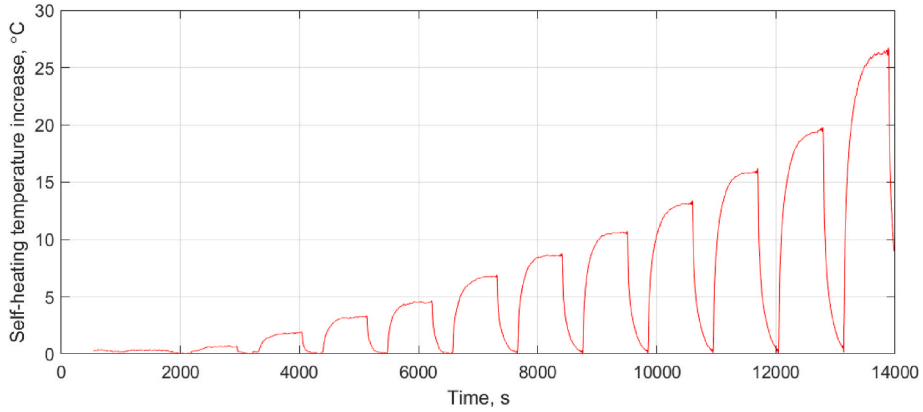

Fig. 4. The exemplary maximal self-heating temperature history plot after processing.

fatigue limit from the intersection of these lines. Since this method introduces man-made uncertainties as stated in Ref. [7], it was assumed that the number of points for interpolation for each line is selected based on the best result of fitting obtained for a given number of interpolated points. This approach finds a confirmation in the numerous previous studies (see, e.g. Refs. [6–8,13,20–22,27,28,55]) to obtain clear bilinear

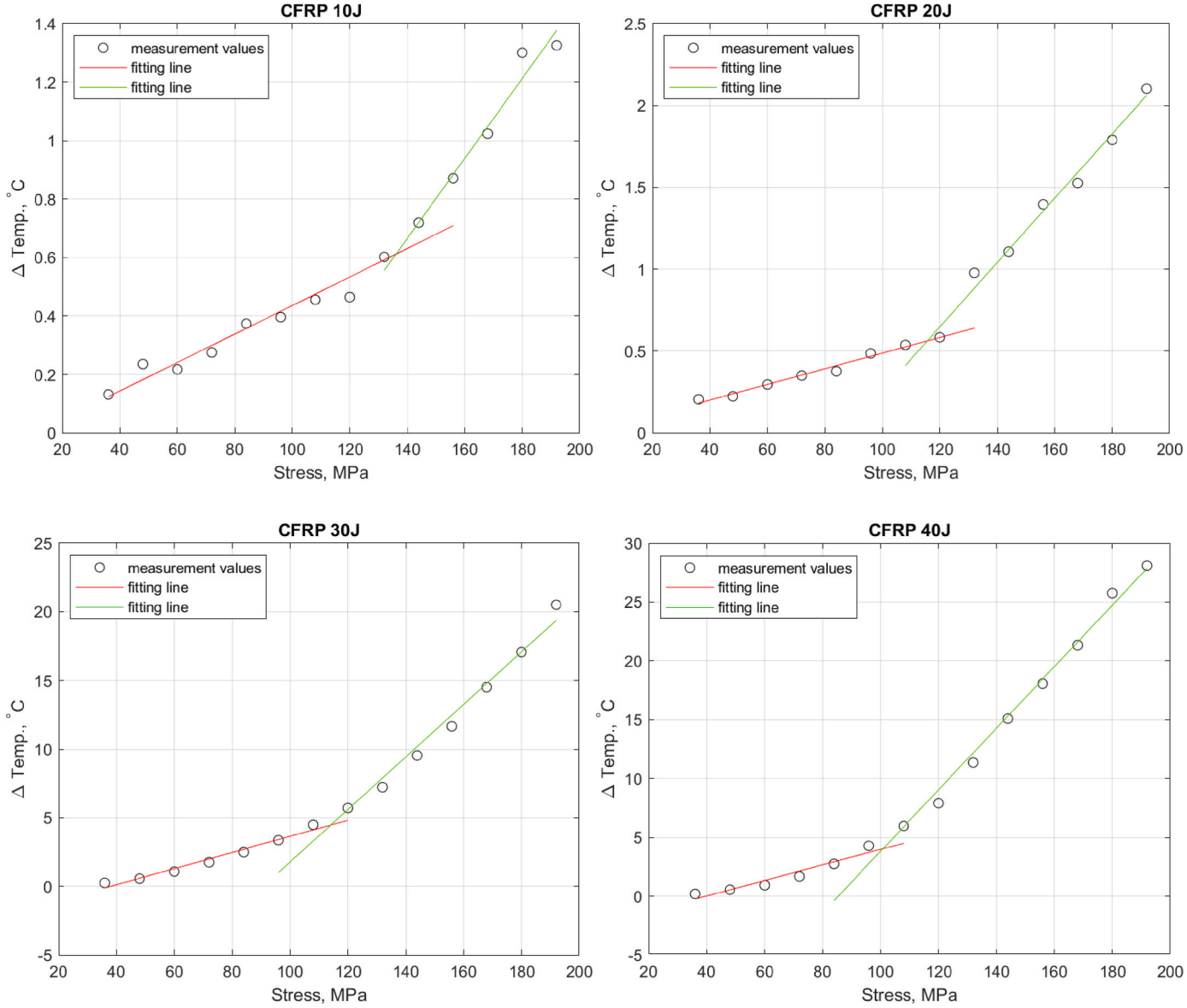

Fig. 5. The selected fatigue limit plots for considered impact energies for CFRP specimens.

behavior. The selected results for the tested specimens are presented in Figs. 5 and 6 for CFRP and GFRP specimens, respectively.

A clear tendency of fatigue limit decreasing with the increase of energy of impact loading is observed on the plots presented in Figs. 5 and 6. It confirms a sensitivity of the approach to a decrease of structural stiffness and more intensive dissipation processes in the composite structures with more widespread LVID. The intensification of dissipation is the result of the appearance of more widespread delamination and more dense network of cracks, and thus a larger area of surfaces participated in friction during cyclic loading. The determined values of the fatigue limit are plotted in Fig. 7, taking into consideration the statistical variations from all tests. The presented results show that the repeatability of the performed tests and the interpolation procedures were very high, which is confirmed by the error bars in Fig. 7 and calculated standard deviation presented in Table 3. Two characteristic drops are observed in both CFRP and GFRP: the drop of fatigue limit due to LVID is the most significant at 20J and 40J. For clarity, the averaged values (Avg.) and their standard deviation (Std.) of the determined fatigue limits using thermographic measurements are presented in Table 3.

From the practical point of view, it is interesting to evaluate a drop of the fatigue limit's character in the light of the ultimate tensile strength (UTS) of the tested composite structures. For this purpose, a ratio of the fatigue limit and UTS was determined (see Table 4).

The results in Table 4 confirm the observations made in Fig. 7 and show how low the fatigue limits are regarding the UTS for the impacted structures. Interestingly, the behavior of both CFRP and GFRP structures with the increasing impact energy is very similar to each other.

3.2. *Influence of location of measurement points of self-heating temperature*

The assessment of the fatigue limit is also proposed using the six-point temperature measurements on the specimen surface throughout the experiments. The response of thermocouples, evolution of the ambient temperature around the specimen and the upper and lower grips temperatures are recorded simultaneously with the time-step of 0.05 s.

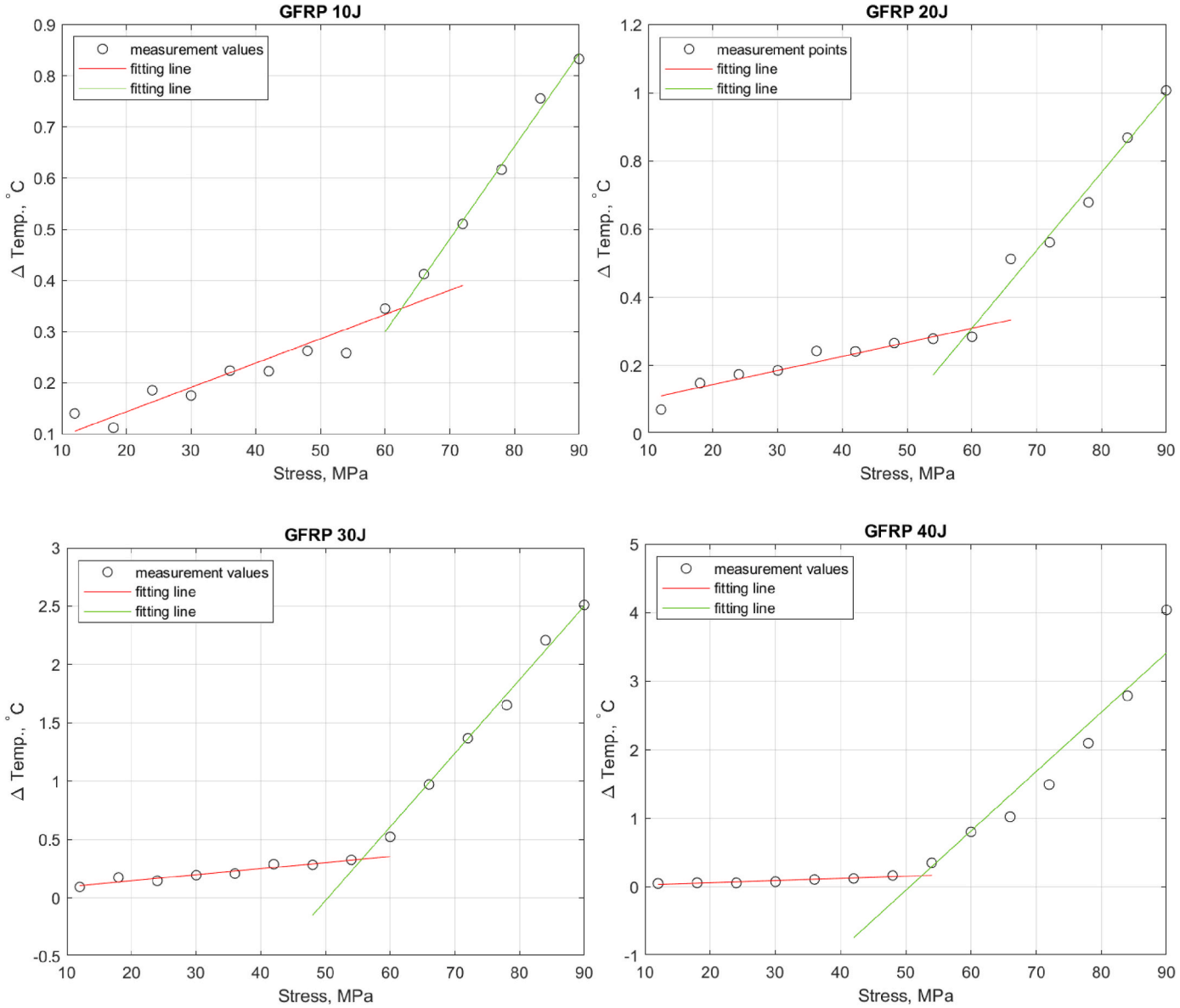

Fig. 6. The selected fatigue limit plots for considered impact energies for GFRP specimens.

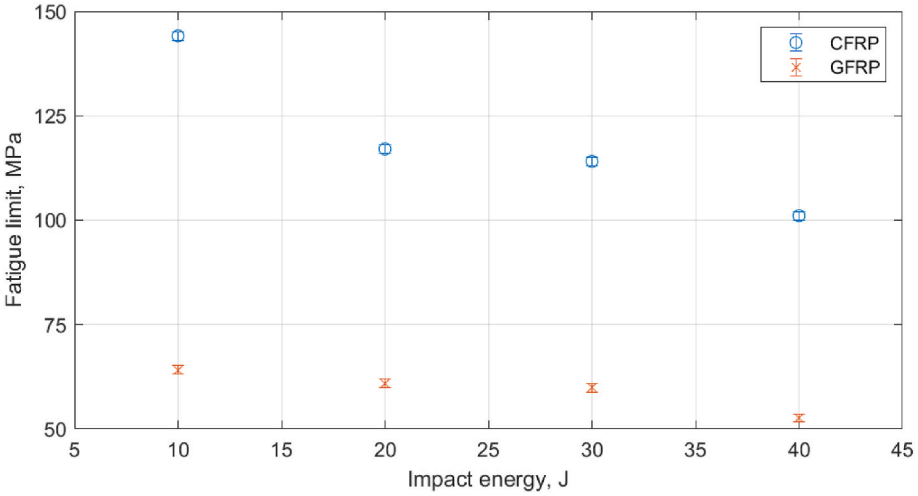

Fig. 7. The fatigue limit values at various impact energies of the tested structures.

Table 3
The averaged fatigue limit values (in MPa) and their standard deviation for the tested specimens.

Impact energy, J	10		20		30		40	
	Avg.	Std.	Avg.	Std.	Avg.	Std.	Avg.	Std.
CFRP	144.12	7.08	117.05	3.30	114.10	4.51	101.09	0.62
GFRP	64.17	1.78	60.97	1.52	59.88	4.27	52.67	0.48

Table 4
The ratios of the fatigue limits to ultimate tensile strength for the tested structures.

Impact energy, J	10	20	30	40
CFRP, -	0.265	0.216	0.210	0.186
GFRP, -	0.155	0.148	0.145	0.127

As in the case of thermograms, the maximal yet stabilized self-heating temperature at each loading level is considered for the fatigue limit estimation. Hence, the representative temperature of each loading block is extracted during its last cycle. Nevertheless, it is to be corrected by cause of the constant rise of ambient temperature in the experimental laboratory. The increase of the self-heating temperature is estimated according to the following equation:

$$\Delta T_i = T_i^{TC} - T_0^{TC} - (T_i^{amb} - T_0^{amb}) \tag{1}$$

where T stands for the temperature, the subsctipts 0 and i for the onset of loading and the end of each loading block measured on the specimen surface by any thermocouple, while the superscripts *TC* and *amb* for thermocouple and ambient, respectively. The rise of the self-heating temperature in six *TC* locations (see Fig. 2(b)) versus stress levels is illustrated in Fig. 8 (CFRP) and 9 (GFRP) for the studied impact energies. Similarly, Luong's method was applied to detect fatigue limit using the same number of points for interpolation for each line as for thermograms. The values were calculated for each thermocouple and each impact energy considered in this study to evaluate the differences in estimated fatigue limits using the previously presented method. The obtained values for fatigue limits for six *TC* locations and average temperature values for thermocouples are stored in Table 5, while Figs. 8 and 9 represent the results of interpolation for average temperature values only.

From the results presented in Figs. 8 and 9, one can observe the differences in measured temperature values, which result from a non-uniformity of the self-heating temperature distributions that emerged from the presence of impact damage. This non-uniformity can be explained by two phenomena: a local stiffness decrease due to impact damage, and thus, higher stress concentration in the neighborhood of this damage as well as frictional heating in the impacted region. Analyzing the fatigue limits determined for particular thermocouples (see Table 5), one can observe that the differences in estimated fatigue limits are generally low, resulting from already mentioned stiffness reduction and frictional heating, which is additionally confirmed by low standard deviation (Std.) values. However, one can also observe a decreasing tendency of the fatigue limit with the increasing impact energy for all thermocouples within a given case. When analyzing fatigue limit values determined for averaged temperature, this is especially well visible.

Comparing the fatigue limits determined from measurements using thermocouples (Table 5) with the results from thermographic measurements (Table 3), one can conclude that the obtained values reveal the high similarity between the applied measurement methods, which is confirmed by statistical analysis. The underestimation observed for the results obtained from measurements using thermocouples can be explained by a possibility of measuring temperature evolution using an IR camera precisely at the center of impact damage, where the temperature was the highest, while measurements using thermocouples were performed in the vicinity of this damage. The mentioned physical phenomena that explain the non-uniformity of temperature distribution also influenced the determined temperature values for particular loading blocks and, consequently, the slopes of interpolation lines.

The fatigue limit results, computed using thermocouples, are represented versus impact energy in Fig. 10. The analysis of Figs. 7 and 10 point out the close resemblance of the fatigue behavior of GFRP for all impact energies (cf. Tables 4 and 6). Like the CFRP specimens, the fatigue limit for 10J appears underrated by 16% compared to the IRT method, whereas a slight overestimation by 5% and 7% occurs at 30J and 40J, respectively. The reasons of the observed differences in results are the same as for the differences in the estimation of fatigue limits presented above.

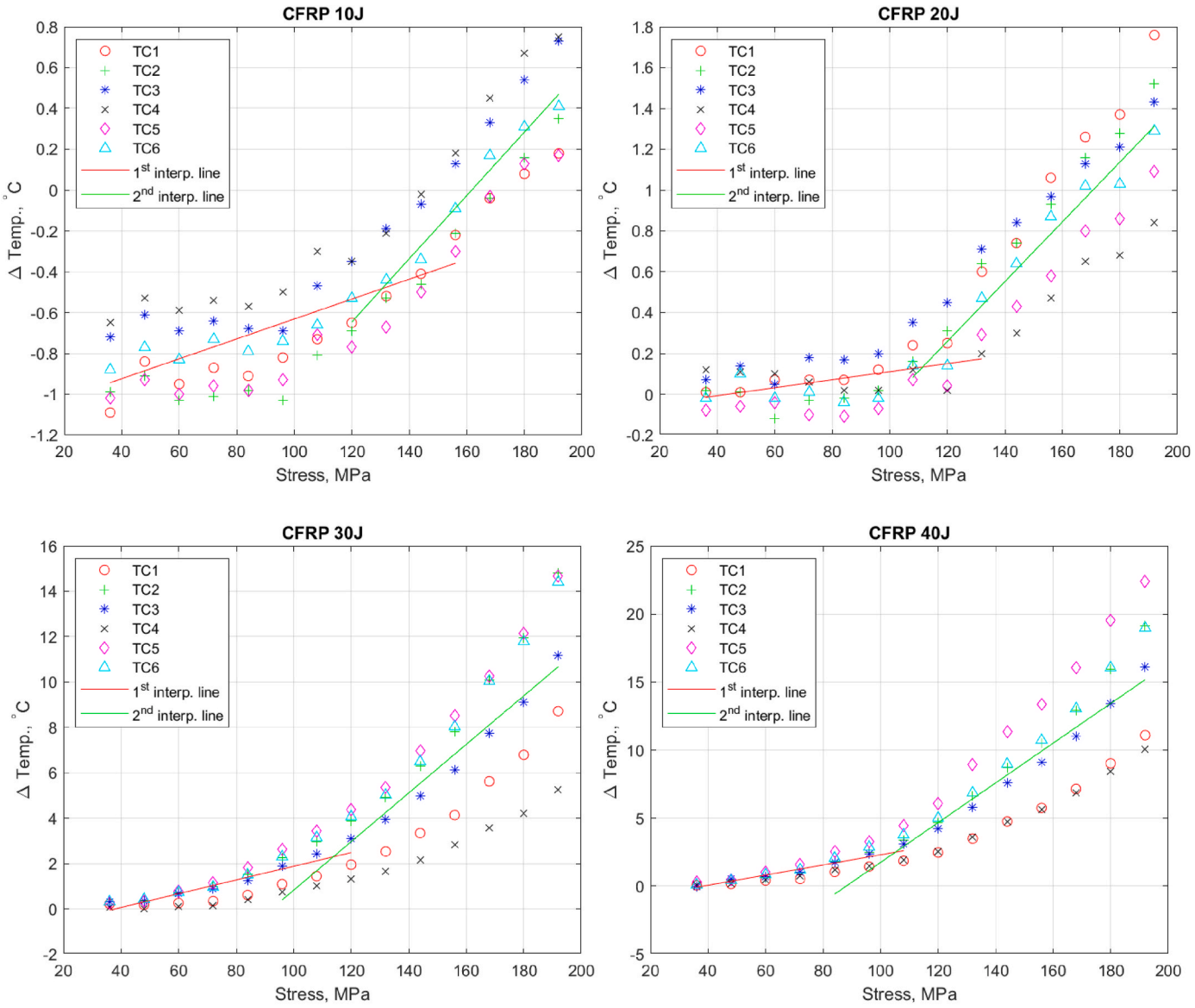

Fig. 8. The selected fatigue limit plots for considered impact energies for CFRP specimens using thermocouples.

3.3. Identification of impact damage

3.3.1. Detectability of impact damage from IRT

The experimental setup presented in section 2.3 enables detecting, localizing, and identifying LVID in the tested specimens. Using an IR camera for continuous registration of a thermal response on a tested structure creates a possibility of hybridization to evaluate the fatigue limit of a structure, such as described in sections 3.1 and 3.2. It also permits performing NDT on a tested structure by identifying impact damage presence and its extent. Such a possibility is especially important in the presence of BVID and visible impact damage (VID) when the internal damage is not visible on the surface. Such examples are presented in Fig. 11 for heavily damaged specimens, where the full damage extent is not clearly visible on the tested structure's surface (see Fig. 1 (b)). The CFRP specimens with VID of 30J and 40J, respectively, were considered in the presented cases. In each case, the thermograms were selected from the beginning of the 10th loading block when the loading and the resulting heating rates were sufficiently high. The idea behind this approach is similar to the SHVT method described in detail in numerous previous publications (see Refs. [33,51–53] for instance), where the thermal excitation of a polymeric or PMC structure is performed by an initiation of the self-heating effect, induced by mechanical loading.

As observed, the regions with the higher self-heating temperature are more prominent than the damaged regions visible on the surfaces of the considered specimens (cf. Figs. 1(b) and 11). Therefore, it indicates the presence of internal damage in these specimens. In particular, besides the hot spots in Fig. 11, which coincide with indentations made by the impactor, one can observe the regions with lower temperatures (represented on the thermograms by colors different than grey and a black color), which may represent cracks and delamination inside a structure. It is important to mention that there is no strict dependency between damage and specific colors representing it, since the color scaling depends on the heating level of a specimen. However, the determination of damage presence and location can be performed based on the visible differences in thermal response between damaged and intact regions of a structure.

An X-ray computed tomography (XCT) NDT experiments were performed to confirm expected internal damage for the considered specimens. For this purpose, the XCT scanning system Xradia MicroXCT-400 (Zeiss) equipped with a Hamamatsu 150 kV sealed X-ray source with a variable current from 40 kV to 150 kV was used. The acquisition system

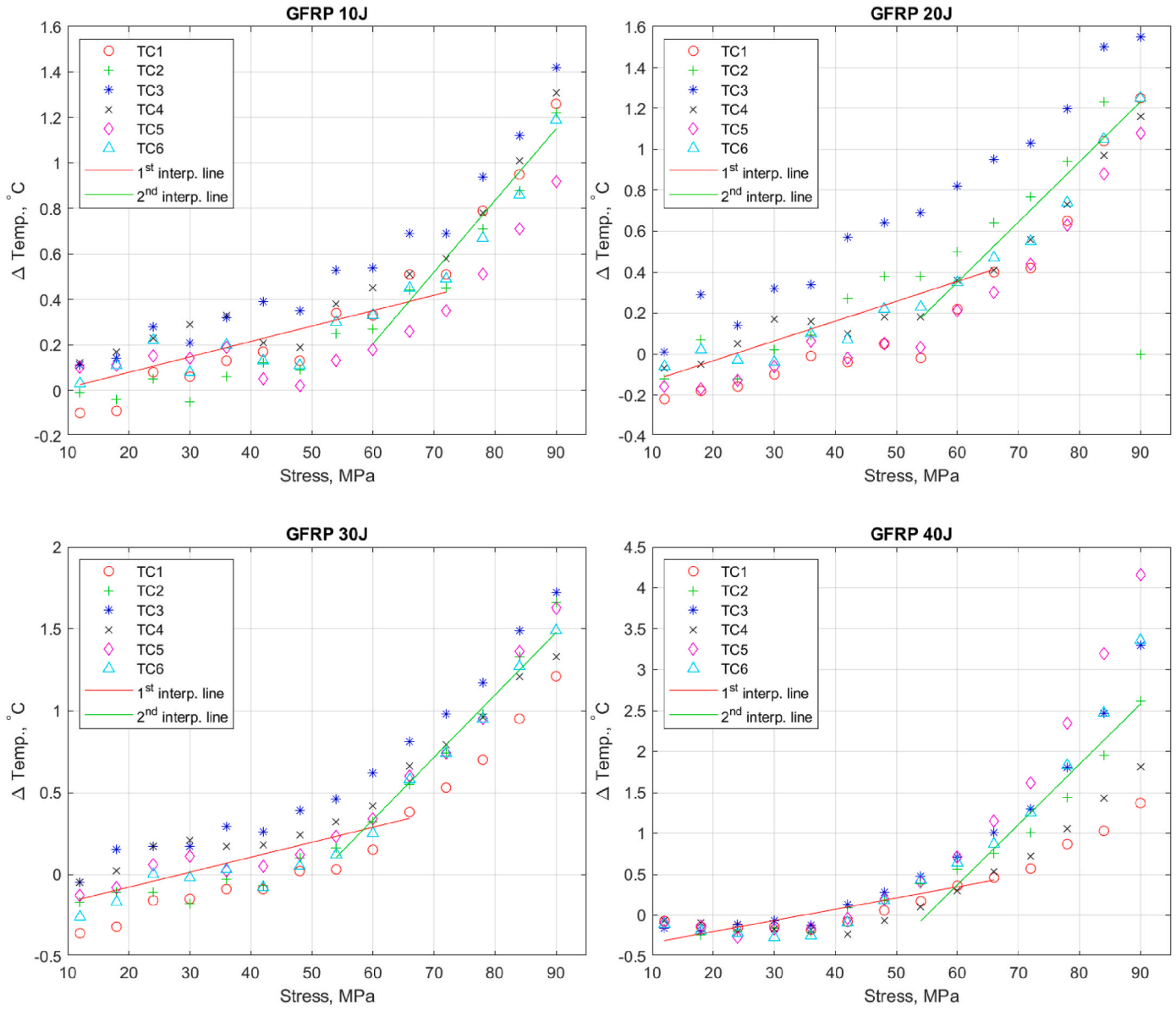

Fig. 9. The selected fatigue limit plots for considered impact energies for GFRP specimens using thermocouples.

Table 5
The determined fatigue limits for measurements with thermocouples.

CFRP								
Impact energy, J	Fatigue limit, MPa							
	TC1	*TC2*	*TC3*	*TC4*	*TC5*	*TC6*	Average	Std.
10	127.27	131.64	131.64	130.91	129.07	131.64	130.55	1.81
20	115.64	114.73	113.76	119.03	113.94	108.09	111.39	3.56
30	114.72	114.42	113.96	113.49	113.19	112.76	113.76	0.75
40	107.09	105.21	105.55	106.58	103.30	105.12	105.16	1.32
GFRP								
10	66.36	65.49	67.30	66.51	64.32	65.62	65.90	1.03
20	59.57	60.61	61.90	60.62	60.12	60.52	60.19	0.77
30	57.30	54.72	55.59	55.10	55.83	55.09	55.53	0.92
40	46.88	50.77	51.51	48.46	51.07	49.73	50.10	1.78

consists of a series of objectives of different magnifications and a CCD detector of 2048 × 2048 pixels. The scanning parameters were as follows: voltage 40 kV, power 8 W, mode Macro-70, and exposure time 15 s. The dimension of a side of a single voxel was 14.22 μm, representing the assumed spatial resolution of the XCT scans. The acquired tomograms were then post-processed with the dedicated software Xm Reconstructor (Carl Zeiss) and exported in the form of sequences of 2D cross-sections. The 3D views of the scanned specimens with the selected

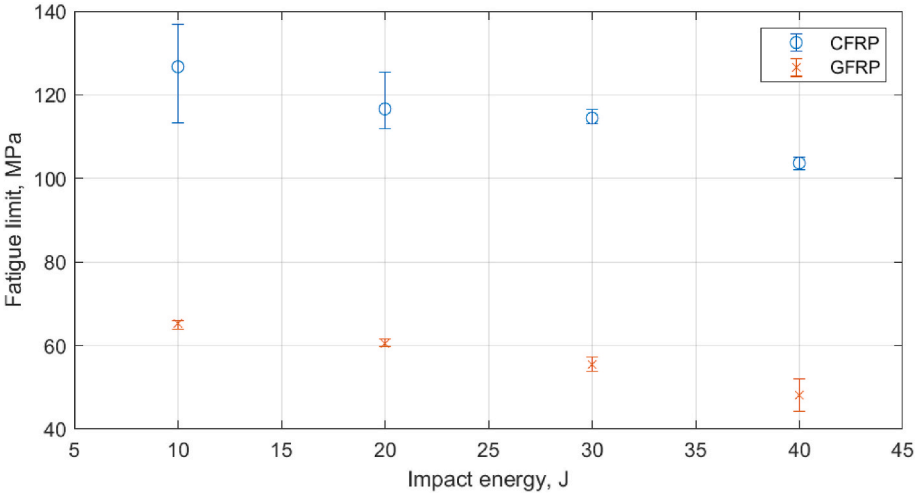

Fig. 10. The fatigue limit values at various impact energies of the tested structures using thermocouples.

Table 6
The ratios of the fatigue limits to ultimate tensile strength for the tested structures.

Impact energy, J	10	20	30	40
CFRP, -	0.223	0.215	0.221	0.200
GFRP, -	0.153	0.144	0.142	0.123

cross-sections through LVID regions are presented in Fig. 12. The dimensions of the scanned area was 25 × 20 mm, where the larger value is the width of the specimen, which was enough to capture LVID.

From the cross-sections presented in Fig. 12, it is clearly visible that the character of damage is typical for low-velocity impact loading of the composite structures, i.e. cracks propagate in a normal direction with respect to the impacted surface, while the area of delamination at particular layers increasing from top to bottom of a structure from the location of impact. Similar failure mechanism is observed in literature (see, e.g. Refs. [38,45]). Besides, it is characterized by a dense net of cracks and delaminated areas, which coincides with the damaged areas observed on thermograms (see Fig. 11). The presented results confirm the possibility of surface and subsurface damage identification caused by low-velocity impact loading as a simultaneous NDT evaluation during fatigue limit testing on composite structures.

3.3.2. *Evaluation of the detectability threshold*

From a practical point of view, it is essential to determine the detectability thresholds of the proposed hybrid method. Such threshold will allow evaluating the necessary stress level to be applied to detect damage with various impact energies for two considered PMC structures and describe the detectability in the form of an impact energy function. According to the character of fatigue limit testing procedure, it is essential to limit the evaluation of the detectability thresholds to the number of a loading block. For this purpose, a perceptual evaluation of thermograms was performed based on shapes of LVID and characteristic

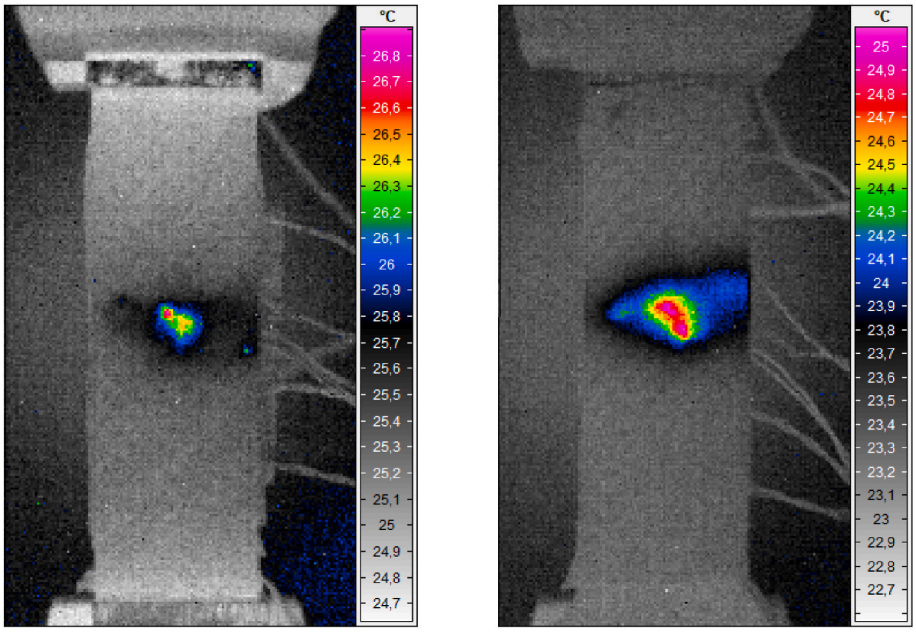

Fig. 11. The exemplary thermograms of the CFRP specimens with (a) 30J and (b) 40J VID.

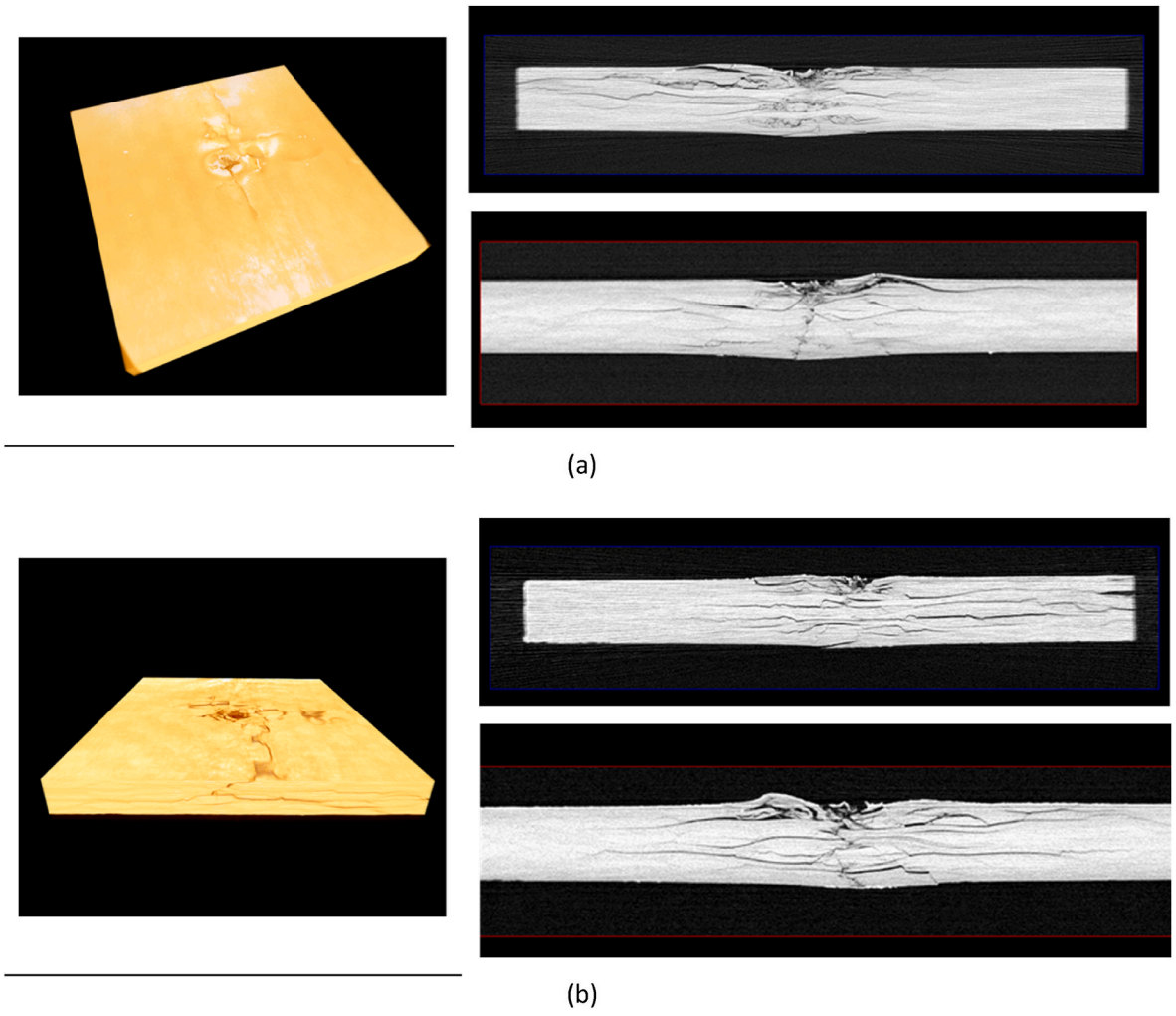

Fig. 12. The 3D views and 2D cross-sections through the center of VID of the tomograms of the CFRP specimens with (a) 30J and (b) 40J VID.

local disturbances observable on the acquired thermograms, i.e. thermal hot spots and areas manifested by color change with respect to intact regions on tested specimens. The detectability was evaluated based on two criteria: I – a local disturbance in the location of LVID, II – the highest temperature registered in the location of LVID. The exemplary thermograms with damage at the earliest stages of LVID visibility for the considered impact energies and materials are presented in Fig. 13. The numbers of loading blocks in which LVID is detectable for all tested specimens are additionally stored in Table 7. The corresponding values of the applied loading can be found in Table 2.

From the results presented in Table 7, one can conclude that LVID is generally well detectable during the fatigue limit tests. The bare detectability was registered for the lowest impact loading; however, the earliest stage of detectability for higher impact energy values is far below the maximal stress levels applied to the tested specimens within the assumed loading blocks (see Table 2 for the detailed values). In such a class of problems, there is always a tradeoff between damage detectability and non-destructivity of the approach, i.e. the increase of loading may significantly improve the detectability of LVID (particularly BVID). However, it may also introduce irreversible changes and, consequently, structural degradation of a tested specimen. Taking this into consideration and also considering the differences observed in Table 7 (resulting from various material properties and various levels of stress), it is expedient to analyze the amount of the self-heating temperature increase for the particular cases being investigated. It is also interesting to include the evaluation of the lowest self-heating temperature increase necessary for detection of LVID according to the two above-described criteria. The results of this analysis are presented in Fig. 14.

The results presented in Fig. 14 clearly show that the increase of the self-heating temperature necessary for detection of LVID is in most cases below 1 °C, which is far below the temperature values obtained during fatigue limit testing. Additionally, according to the previous studies on the criticality of the self-heating effect [33], the above-presented results confirm the non-destructive character of evaluation of LVID using the proposed approach. Further improvement of LVID detectability is possible by applying image processing techniques to the acquired thermograms. The performance of selected techniques was presented in Ref. [53].

4. Discussion and conclusions

The influence of LVID on the fatigue limit of CFRP and GFRP structures was investigated in this study. It was demonstrated a decreasing tendency of fatigue limit with an increased energy of impact loading for both tested materials using two measurement techniques, which were based on using IR camera and thermocouples. The obtained results manifested low discrepancies between the obtained results for various measurements methods in estimation of fatigue limits, i.e. the results obtained from measurements using thermocouples are, in general, underrated compared to results obtained for IRT. The observed differences come from the non-uniformity of the self-heating temperature distributions due to the presence of impact damage and the difficulty of

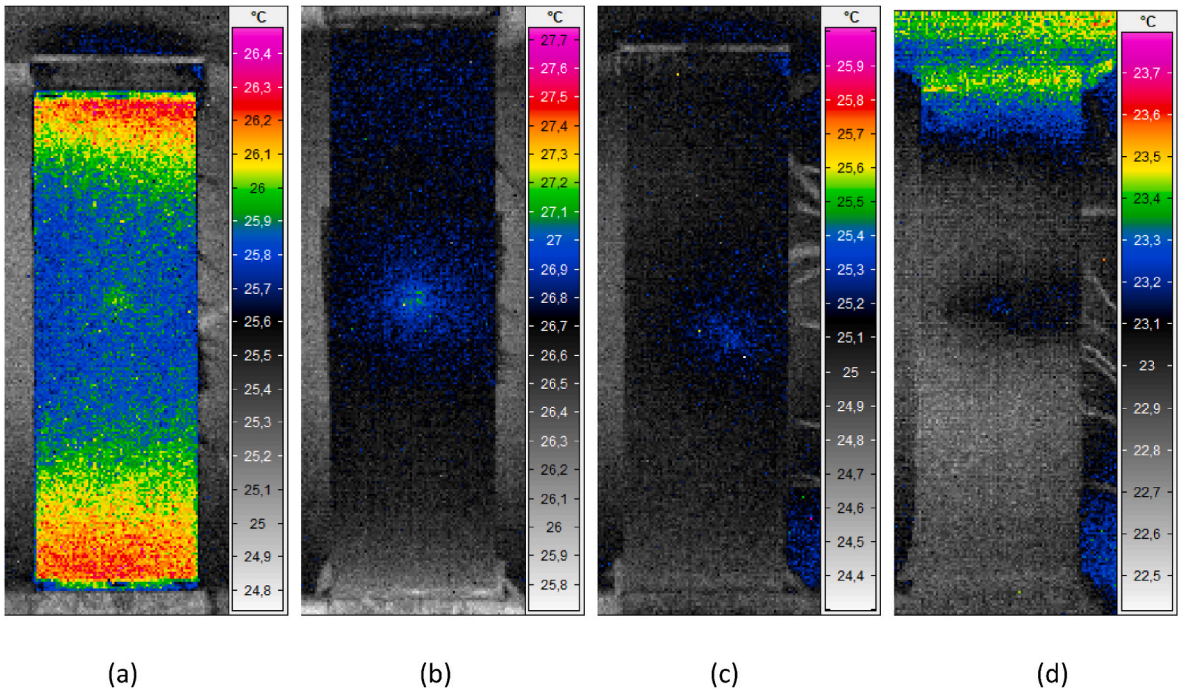

Fig. 13. Exemplary thermograms with detected LVID at the earliest stage for (a) 10J, (b) 20J, (c) 30J, and (d) 40J of impact energy for CFRP specimens.

Table 7
The loading block numbers per specimen manifesting detectability of LVID in CFRP and GFRP specimens during fatigue limit tests.

Impact energy, J	10			20			30			40		
Criterion I, loading block numbers *i*												
Specimen no.	1	2	3	1	2	3	1	2	3	1	2	3
CFRP	13	14	14	8	8	6	1	1	1	1	1	1
GFRP	–	–	–	8	12	14	7	7	8	5	5	5
Criterion II, loading block numbers *i*												
Specimen no.	1	2	3	1	2	3	1	2	3	1	2	3
CFRP	–	–	–	10	9	9	1	2	2	2	2	2
GFRP	–	–	–	10	14	–	9	9	9	7	7	7

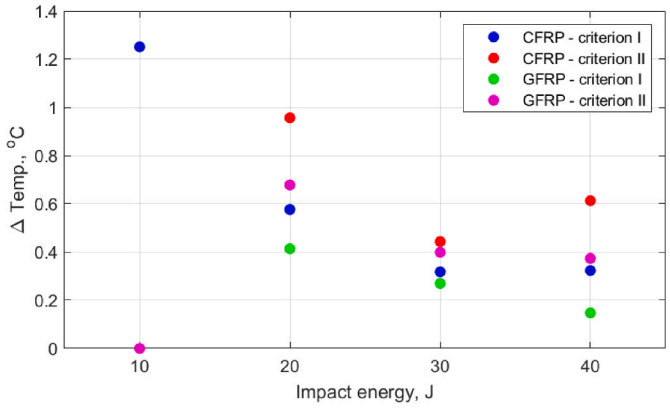

Fig. 14. The minimal self-heating temperature increase required for the detection of LVID.

measuring the evolution of peak temperature values in the location of this damage using thermocouples. It is due to the difficulties in evaluating the thermal hot spot in the location of impact damage and proper mounting a thermocouple on a damaged surface. It is thus essential to place a thermocouple during self-heating tests close to a location of expected damage to obtain the most accurate results. Nevertheless, if a damage location is unknown, the estimation of fatigue limit is still possible with a quite high accuracy, which was confirmed during the study (see Table 5). The obtained results confirmed that measurements using thermocouples could successfully substitute expensive measurements using an IR camera with an acceptable level of accuracy. However, it should be considered that such a measurement technique underestimates the results.

The observed differences in the thermal response of CFRP and GFRP structures result from different susceptibility of these structures to withstand impact damage and, consequently, different failure mechanisms. As it can be seen in Fig. 1(b), in the case of GFRP structures, impact loading did not cause extensive delamination (which was observed via light transmission visual inspection), while in the case of CFRP, this delamination was significant, which is recognizable both in Fig. 1(b) and found a confirmation during X-ray CT tests (see Fig. 12). It is due to the higher fragility of CFRP structures than GFRP ones which implies non-symmetric temperature distributions (see Figs. 11 and 13, for instance). Besides, it influences the measured temperature values and determined fatigue limits at the end.

The analysis of the observed differences in measurements of low-energy impacts (10J and 20J) for both tested materials show a significant influence of changes of environmental temperature, which need to be controlled, especially in such cases. The proposed hybrid approach can overcome this deficiency of classical fatigue limit estimation. The simultaneous determination of fatigue limit together with the evaluation of damage using self-heating-based vibrothermography allows identifying not only a decrease of a fatigue limit but also identifying a damage

location and shape, which also confirms its presence. Moreover, as it was presented in section 3.3.2, an only slight increase of self-heating temperature (up to 1 °C as can be seen in Fig. 14) ensures the detectability of damage in a non-destructive way, considering the criteria of the criticality of the self-heating effect (see Refs. [31,33] for more details).

The proposed approach has other advantages: the comprehensive and non-destructive analysis of a structural condition is possible without a necessity in a healthy reference structure. The performed analysis is significantly faster than classical fatigue testing, where several specimens are required to build an S–N curve [56,57]. The suggested approach is then competitive for applications in industrial conditions.

Knowing the material properties of a tested structure, it is possible to evaluate the structural residual life, as demonstrated in this paper. It draws new directions of continuing these research studies, mainly to evaluate the strain evolution in the damaged area and its connection with the amount of dissipated energy. An investigation of appearing thermoviscoelastic and thermoviscoplastic phenomena during cyclic loading could also be studied.

CRediT author statement

Andrzej Katunin: Conceptualization, Methodology, Software, Validation, Formal analysis, Investigation, Resources, Data Curation, Writing - Original Draft, Writing - Review & Editing, Supervision, Visualization, Funding acquisition. **Ivanna Pivdiablyk:** Conceptualization, Methodology, Validation, Formal analysis, Investigation, Data Curation, Writing - Original Draft, Writing - Review & Editing, Visualization. **Laurent Gornet:** Conceptualization, Methodology, Investigation, Resources, Formal analysis, Writing - Review & Editing. **Patrick Rozycki:** Conceptualization, Methodology, Formal analysis, Writing - Review & Editing.

Declaration of competing interest

The authors declare that they have no known competing financial interests or personal relationships that could have appeared to influence the work reported in this paper.

Acknowledgments

Andrzej Katunin would like to acknowledge the Embassy of France in Warsaw for the financial support of the research internship implemented in the École Centrale de Nantes within the French Government Scholarship (BGF) for Polish researchers granted in 2021. The authors would like to thank François Bertrand from the École Centrale de Nantes for performing X-ray computed tomography scans in this study.

References

[1] Fish J, Yu Q. Computational mechanics of fatigue and life predictions for composite materials and structures. Comput Methods Appl Mech Eng 2002;191:4827–49.
[2] Lachihab A, Sab K. Does a representative volume element exist for fatigue life prediction? The case of aggregate composites. Int J Numer Anal Methods GeoMech 2008;32:1005–21.
[3] Naderi M, Maligno AR. Fatigue life prediction of carbon/epoxy laminates by stochastic numerical simulation. Compos Struct 2012;94:1052–9.
[4] Sørensen BF, Goutianos S. Micromechanical model for prediction of the fatigue limit for unidirectional fibre composites. Mech Mater 2019;131:169–87.
[5] Xiong J, Zhu Y, Luo C, Li Y. Fatigue-driven failure criterion for progressive damage modelling and fatigue life prediction of composite structures. Int J Fatig 2021;145:106110.
[6] Huang J, Li C, Liu W. Investigation of internal friction and fracture fatigue entropy of CFRP laminates with various stacking sequences subjected to fatigue loading. Thin-Walled Struct 2020;155:106978.
[7] Huang J, Pastor M-L, Garnier C, Gong X. Rapid evaluation of fatigue limit on thermographic data analysis. Int J Fatig 2017;104:293–301.
[8] Luong MP. Fatigue limit evaluation of metals using an infrared thermographic technique. Mech Mater 1998;28:155–63.
[9] La Rosa G, Risitano A. Thermographic methodology for rapid determination of the fatigue limit of materials and mechanical components. Int J Fatig 2000;22:65–73.
[10] Fargione G, Geraci A, La Rosa G, Risitano A. Rapid determination of the fatigue curve by the thermographic method. Int J Fatig 2002;24:11–9.
[11] Zhang L, Liu XS, Wu SH, Ma ZQ, Fang HY. Rapid determination of fatigue life based on temperature evolution. Int J Fatig 2013;54:1–6.
[12] Liakat M, Khonsari MM. Rapid estimation of fatigue entropy and toughness in metals. Mater Des 2014;62:149–57.
[13] Guo Q, Guo X, Fan J, Syed R, Wu C. An energy method for rapid evaluation of high-cycle fatigue parameters based on intrinsic dissipation. Int J Fatig 2015;80:136–44.
[14] Ricotta M, Meneghetti G, Atzori B, Risitano G, Risitano A. Comparison of experimental thermal methods for the fatigue limit evaluation of a stainless steel. Metals 2019;9:677.
[15] Colombo C, Vergani L. Thermographic applications for the rapid estimation of fatigue limit. Procedia Struct Integr 2019;24:658–66.
[16] Hajshirmohammadi B, Khonsari MM. A simple approach for predicting fatigue crack propagation rate based on thermography. Theor Appl Fract Mech 2020;107:102534.
[17] Karama M. Determination of the fatigue limit of a carbon/epoxy composite using thermographic analysis. Struct Control Health Monit 2011;18:781–9.
[18] Meneghetti G, Quaresimin M. Fatigue strength assessment of a short fiber composite based on the specific heat dissipation. Compos B Eng 2011;42:217–25.
[19] Jegou L, Marco Y, Le Saux V, Calloch S. Fast prediction of the Wöhler curve from heat build-up measurements on Short Fiber Reinforced Plastic. Int J Fatig 2013;47:259–67.
[20] Montesano J, Fawaz Z, Bougherara H. Use of infrared thermography to investigate the fatigue behavior of a carbon fiber reinforced polymer composite. Compos Struct 2013;97:76–83.
[21] Kordatos EZ, Dassios KG, Aggelis DG, Maikas TE. Rapid evaluation of the fatigue limit in composites using infrared lock-in thermography and acoustic emission. Mech Res Commun 2013;54:14–20.
[22] Shah OR, Tarfaoui M. Effect of damage progression on the heat generation and final failure of a polyester–glass fiber composite under tension–tension cyclic loading. Compos B Eng 2014;62:121–5.
[23] Peyrac C, Jollivet T, Leray N, Lefebvre F, Westphal O, Gornet L. Self-Heating method for fatigue limit determination on thermoplastic composites. Procedia Eng 2015;133:129–35.
[24] Montesano J, Fawaz Z, Bougherara H. Non-destructive assessment of the fatigue strength and damage progression of satin woven fiber reinforced polymer matrix composites. Compos B Eng 2015;71:122–30.
[25] Palumbo D, De Finis R, Demelio PG, Galietti U. A new rapid thermographic method to assess the fatigue limit in GFRP composites. Compos B Eng 2016;103:60–7.
[26] Gornet L, Sudevan D, Rozycki P. A study of various indicators to determine the fatigue limit for woven carbon/epoxy composites under self heating methodology. Procedia Eng 2018;213:161–72.
[27] Huang J, Garnier C, Pastor M-L, Gong X. A new model for fatigue life prediction based on infrared thermography and degradation process for CFRP composite laminates. Int J Fatig 2019;120:87–95.
[28] Huang J, Garnier C, Pastor M-L, Gong X. Investigation of self-heating and life prediction in CFRP laminates under cyclic shear loading condition based on the infrared thermographic data. Eng Fract Mech 2020;229:106971.
[29] Renshaw J, Chen JC, Holland SD, Thompson RB. The sources of heat generation in vibrothermography. NDT&E Int. 2011;44:736–9.
[30] Katunin A. Domination of self-heating effect during fatigue of polymeric composites. Procedia Struct Integr 2017;5:93–8.
[31] Katunin A, Wronkowicz A, Bilewicz M, Wachla D. Criticality of self-heating in degradation processes of polymeric composites subjected to cyclic loading: a multiphysical approach. Arch Civ Mech Eng 2017;17:806–15.
[32] Katunin A, Wronkowicz A. Characterization of failure mechanisms of composite structures subjected to fatigue dominated by the self-heating effect. Compos Struct 2017;180:1–8.
[33] Katunin A. Criticality of the self-heating effect in polymers and polymer matrix composites during fatigue, and their application in non-destructive testing. Polymers 2019;11:19.
[34] Katunin A, Wachla D. Determination of fatigue limit of polymeric composites in fully reversed bending loading mode using self-heating effect. J Compos Mater 2019;53:83–91.
[35] Nsengiyumva W, Zhong S, Lin J, Zhang Q, Zhong J, Huang Y. Advances, limitations and prospects of nondestructive testing and evaluation of thick composites and sandwich structures: a state-of-the-art review. Compos Struct 2021;256:112951.
[36] Bingol OR, Schiefelbein B, Grandin RJ, Holland SD, Krishnamurthy A. An integrated framework for solid modeling and structural analysis of layered composites with defects. Comput Aided Des 2019;106:1–12.
[37] Hauffe A, Hähnel F, Wolf K. Comparison of algorithms to quantify the damaged area in CFRP ultrasonic scans. Compos Struct 2020;235:111791.
[38] Katunin A, Wronkowicz-Katunin A, Danek W, Wyleżoł M. Modeling of a realistic barely visible impact damage in composite structures based on NDT techniques and numerical simulations. Compos Struct 2021;267:113889.
[39] Wang XG, Crupi V, Guo XL, Zhao YG. Quantitative thermographic methodology for fatigue assessment and stress measurement. Int J Fatig 2010;32:1970–6.
[40] Foti P, Santonocito D, Ferro P, Risitano G, Berto F. Determination of fatigue limit by static thermographic method and classic thermographic method on notched specimens. Procedia Struct Integr 2020;26:166–74.
[41] Schmutzler H, Alder M, Kosmann N, Wittich H, Schulte K. Degradation monitoring of impact damaged carbon fibre reinforced polymers under fatigue loading with pulse phase thermography. Compos B Eng 2014;59:221–9.

[42] Kosmann N, Riecken BT, Schmutzler H, Knoll JB, Schulte K, Fiedler B. Evaluation of a critical impact energy in GFRP under fatigue loading. Compos Sci Technol 2014;102:28–34.
[43] Butler R, Almond DP, Hunt GW, Hu B, Gathercole N. Compressive fatigue limit of impact damaged composite laminates. Compos Appl Sci Manuf 2007;38:1211–5.
[44] Fotouhi M, Damghani M, Leong MC, Fotouhi S, Jalalvand M, Wisnom MR. A comparative study on glass and carbon fibre reinforced laminated composites in scaled quasi-static indentation tests. Compos Struct 2020;245:112327.
[45] Lai WL, Saeedipour H, Goh KL. Mechanical properties of low-velocity impact damaged carbon fibre reinforced polymer laminates: effects of drilling holes for resin-injection repair. Compos Struct 2020;235:111806.
[46] Dziendzikowski M, Kurnyta A, Dragan K, Klysz S, Leski A. In situ Barely Visible Impact Damage detection and localization for composite structures using surface mounted and embedded PZT transducers: a comparative study. Mech Syst Signal Process 2016;78:91–106.
[47] Fierro GPM, Ginzburg D, Ciampa F, Meo M. Imaging of barely visible impact damage on a complex composite stiffened panel using a nonlinear ultrasound stimulated thermography approach. J Nondestr Eval 2017;36:69.
[48] Segers J, Kersemans M, Hedayatrasa S, Calderon J, Van Paepegem W. Towards in-plane local defect resonance for non-destructive testing of polymers and composites. NDT&E Int. 2018;98:130–3.
[49] Zhang X, Wu X, He Y, Yang S, Chen S, Zhang S, Zhou D. CFRP barely visible impact damage inspection based on an ultrasound wave distortion indicator. Compos B Eng 2019;168:152–8.
[50] Lai WL, Saeedipour H, Goh KL. Experimental assessment of drilling-induced damage in impacted composite laminates for resin-injection repair: influence of open/blind hole-hole interaction and orientation. Compos Struct 2021;271:114153.
[51] Katunin A. A concept of thermographic method for non-destructive testing of polymeric composite structures using self-heating effect. Sensors 2018;18:74.
[52] Katunin A, Wachla D. Analysis of defect detectability in polymeric composites using self-heating based vibrothermography. Compos Struct 2018;201:760–5.
[53] Katunin A, Wronkowicz-Katunin A, Wachla D. Impact damage assessment in polymer matrix composites using self-heating based vibrothermography. Compos Struct 2019;214:214–26.
[54] Katunin A, Gnatowski A. Influence of heating rate on evolution of dynamic properties of polymeric laminates. Plast. Rubber Compos. 2012;41:233–9.
[55] Li A, Huang J, Zhang C. Enabling rapid fatigue life prediction of short carbon fiber reinforced polyether-ether-ketone using a novel energy dissipation-based model. Compos Struct 2021;272:114227.
[56] Burhan I, Kim HS. S-N curve models for composite materials characterization: an evaluative review. J. Compos. Sci. 2018;2:38.
[57] Voudouris G, Di Maio D, Sever IA. Experimental fatigue behaviour of CFRP composites under vibration and thermal loading. Int J Fatig 2020;140:105791.